*Structural Engineering and Mechanics, Vol. 25, No. 5 (2007) 613-629*
DOI: http://dx.doi.org/10.12989/sem.2007.25.5.613


# Static and vibration analysis of thin plates by using finite element method of B-spline wavelet on the interval

Jiawei Xiang†

*School of Mechantronic Engineering, Guilin University of Electronic Technology, Guilin 541004, P.R. China*

Zhengjia He‡, Yumin He‡† and Xuefeng Chen‡‡

*School of Mechanical Engineering, Xi'an Jiaotong University, Xi'an 710049, P.R. China*

*(Received August 2, 2005, Accepted September 19, 2006)*

**Abstract.** A finite element method (FEM) of B-spline wavelet on the interval (BSWI) is used in this paper to solve the static and vibration problems of thin plate. Instead of traditional polynomial interpolation, the scaling functions of two-dimensional tensor product BSWI are employed to construct the transverse displacements field. The method combines the accuracy of B-spline functions approximation and various basis functions for structural analysis. Some numerical examples are studied to demonstrate the proposed method and the numerical results presented are in good agreement with the solutions of other methods.

**Keywords:** B-spline wavelet on the interval; finite element method; thin plate analysis; modal analysis.

## 1. Introduction

Wavelet analysis is a new method developed in recent years (Mallat 1999). The wavelet method can be viewed as a method in which the approximating function is defined by use of a multiresolution technique based on scaling or wavelet functions, similar to those used in signal and image processing (Mallat 1999). Its desirable advantages are multi-resolution properties and various basis functions for structural analysis. By means of "two-scale relations" of scaling functions, the scale adopted can be changed freely according to requirements to improve analysis accuracy. So wavelet method is well argued by many researchers not only in numerical analysis domains (Canuto 1999, 2000, Cohen 2003) but also in structural analysis fields (Chen 1995, 1996, Zhou, Ko 1997, 1998, Basu 2003, Ma 2003, Chen 2004, Xiang 2006). Basu indicated that the finite difference and Ritz type methods of the pre-computer era had largely been replaced in the computer era by FEM, boundary element method (BEM), Meshless method, and in the near future it may be the turn for

† Lecturer, Corresponding author, E-mail: wxw8627@163.com
‡ Professor, E-mail: hzj@mail.xjtu.edu.cn
‡‡ Doctoral student, E-mail: heyumin@mailst.xjtu.edu.cn
‡‡ Lecturer, E-mail: cxf@mail.xjtu.edu.cn

wavelet method (Basu 2003). Recently, one-dimensional Daubechies wavelet Euler beam element had been constructed (Ma 2003). And the two-dimensional Daubechies wavelet element for a thin plate-bending problem had also been constructed (Chen 2004). However, for Daubechies wavelets lacking of the explicit function expression, traditional numerical integrals such as Gauss integrals cannot provide desirable precision, the key problem is to calculate connection coefficients (Ma 2003, Chen 2004) when the Daubechies scaling and wavelet functions are employed to construct wavelet FEM solving equations. Since the connection coefficients derivation can only be obtained for integration in global coordinates, it will fail when the integrand involves variant Jacobians (Chen 1995, 1996). Moreover, the connection coefficients calculation is a complex process, which will increases the coding work and calculating costs.

In the construction of wavelet-based FEM solving equations, instead of traditional polynomial interpolation, scaling and wavelet functions have been adopted, which embodied with the prominent advantage that the B-spline wavelets on the interval have explicit expressions (Xiang 2006). So the element stiffness or mass matrix can be calculated conveniently. Furthermore, B-spline wavelets have the best approximation properties among all known wavelets of a given order $L$ (Cohen 2003). However, the originally spline wavelets are defined on the whole real space. Using the wavelets defined on the whole real space as interpolating functions will bring the instability phenomenon (Bertoluzza 1994). To overcome this limitation, Chui and Quak constructed BSWI functions, and presented the corresponding fast decomposition and reconstruction algorithm (Chui 1992, Quak 1994). Goswami, Chan and Chui also used the BSWI solving the first-kind integral equations (Goswami 1995). The wavelets on a bounded interval have limited dimension towards every scaling and wavelet space. So any functions on the interval will be expanded as a sum of finite-dimensional wavelet series, which plays a very important role in constructing element-interpolating functions because it is easy to apply wavelets or scaling functions to FEM. Moreover, the application of the B-spline wavelets basis to the versatile finite element method provides accurate analytical results and a robust multi-level solving process (Canuto 1999, 2000). Since the cubic B-spline interpolated functions have sufficient continuity and are piecewise polynomial, so the B-spline FEM gives accurate results than traditional FEM (Shen 1991, 1995).

The aim of this paper is three-fold. Firstly, instead of traditional polynomial, the tensor product BSWI scaling functions are adopted to form FEM BSWI solving equations. Secondly, Based on the generalized function of potential energy and variation principle, the FEM BSWI solving equations are given for static and free vibration analysis of rectangle and skew plates. Finally, Some numerical examples are given and the numerical results of presented method have been compared with the published solutions.

## 2. Two-dimensional tensor product BSWI

B-spline functions for a given simple knot sequence can be constructed by taking piecewise polynomials between the knots and joining them together at the knots in such a way as to obtain a certain order of overall smoothness. B-splines of $m$th order are in $C^{m-2}$. Since the function $f(x)$ on the interval $[a, b]$ can be mapped to the standard interval $[0, 1]$ by the transformation formula $\xi = (x-a)/(b-a)$, it only needs to construct $m$th order B-spline function space on the interval $[0, 1]$. Generally, the interval $[0, 1]$ can be divided into $2^j$, ($j \in \mathbf{Z}^+$ is the scale) segments, and then increasing $m-1$ knots outside each endpoint and looking the two lateral $m-1$ knots as virtual

multi-knots of the endpoint 0 and 1. Let $\{\xi_k^j\}_{k=-m+1}^{2^j+m-1}$ be a knot sequence with $m$-tuple knots at 0 and 1, then the whole knot numbers are $2^j + 2m - 1$, and the knot sequence form B-spline functions, which can be further constructed to the $m$th order nested B-spline subspace $V_j$. Its basis functions are given below

$$B_{m,k}^j(x) = N_m(2^j\xi - k), \quad (k = -m+1, \ldots, 2^j - 1), \quad \text{supp}B_{m,k}^j = [\xi_k^j, \xi_{m+k}^j] \tag{1}$$

where $N_m(x)$ is cardinal spline function. Let $\phi_{m,k}^j(\xi) = B_{m,k}^j(\xi)$ be the scaling functions of BSWI, we can obtain the multi-resolution analysis (MRA) on the bounded interval [0, 1] (Chui 1992, Quak 1994) and the order of scaling functions $\phi_{m,k}^j(\xi)$ is $m - 1$.

The support of the inner (without multiple knots) B-spline occupies $m$ segments and that of the corresponding semi-orthogonal wavelet occupies $2m - 1$ segments. At any scale $j$, the discretization step is $1/2^j$ which, for $j > 0$, gives $2^j$ number of segments on [0, 1]. Therefore, to have at least one inner wavelet on the interval [0, 1], the following condition must be satisfied.

$$2^j \geq 2m - 1 \tag{2}$$

While 0 scale $m$th order B-spline functions and the corresponding wavelets (Goswami 1995) are given, $j$ scale $m$th order B-spline scaling functions $\phi_{m,k}^j(\xi)$ and the corresponding wavelets $\psi_{m,k}^j(\xi)$ can be evaluated by the following formula

$$\phi_{m,k}^j(\xi) = \begin{cases} \phi_{m,k}^l(2^{j-l}\xi), & k = -m+1, \ldots, -1 \quad \text{(0 boundary scaling functions)} \\ \phi_{m,2^j-m-k}^l(1 - 2^{j-l}\xi), & k = 2^j - m + 1, \ldots, 2^j - 1 \quad \text{(1 boundary scaling functions)} \\ \phi_{m,0}^l(2^{j-l}\xi - 2^{-l}k), & k = 0, \ldots, 2^j - m \quad \text{(inner scaling functions)} \end{cases} \tag{3}$$

$$\psi_{m,k}^j(\xi) = \begin{cases} \psi_{m,k}^l(2^{j-l}\xi), & k = -m+1, \ldots, -1 \quad \text{(0 boundary wavelets)} \\ \psi_{m,2^j-2m-k+1}^l(1 - 2^{j-l}\xi), & k = 2^j - 2m + 2, \ldots, 2^j - m \quad \text{(1 boundary wavelets)} \\ \psi_{m,0}^l(2^{j-l}\xi - 2^{-l}k), & k = 0, \ldots, 2^j - 2m + 1 \quad \text{(inner wavelets)} \end{cases} \tag{4}$$

The wavelets compactly supported intervals are

$$\text{supp}\psi_{m,k}^j(\xi) = \begin{cases} [k2^{-j}, (2m - 1 + k)2^{-j}] & \text{(inner wavelets)} \\ [0, (2m - 1 + k)2^{-j}] & \text{(0 boundary wavelets)} \\ [k2^{-j}, 1] & \text{(1 boundary wavelets)} \end{cases} \tag{5}$$

Let $j_0$ be the scale for which the condition Eq. (2) is satisfied. Then for each $j > j_0$, let $l = 0$, we can get the scaling and wavelet functions easily through Eq. (3) and Eq. (4). There are $m - 1$ boundary scaling functions and wavelets at 0 and 1, and $2^j - m + 1$ inner scaling functions, and $2^j - 2m + 2$ inner wavelets. Fig. 1 shows all the scaling functions and wavelets for $m = 4$ at the scale $j = 3$.

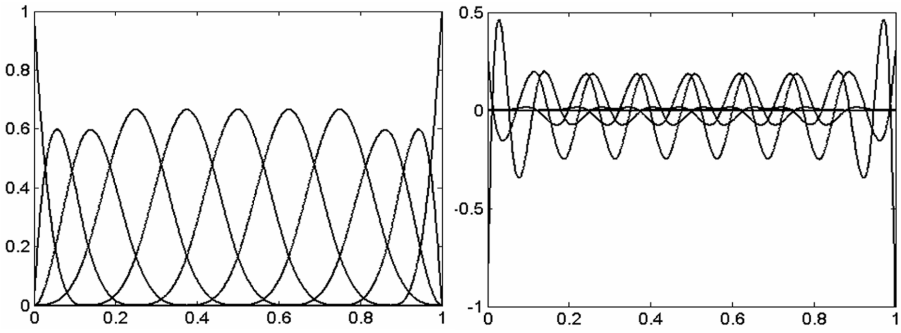


Fig. 1 Scaling functions and wavelets on the interval [0, 1]

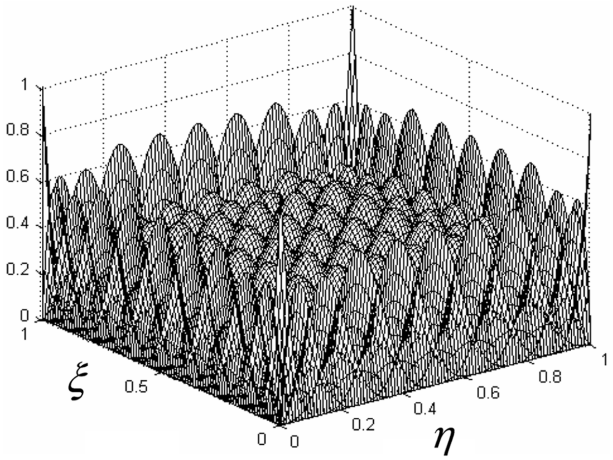


Fig. 2 Tensor product BSWI scaling functions $\varphi = \varphi_1 \otimes \varphi_2$

Tensor product of one-dimensional wavelets (Mallat 1999) is the easy and direct way to construct two-dimensional BSWI. A wavelet semi- orthonormal basis at scale $j$ of $L^2(\mathbf{R}^2)$ is constructed with tensor product of the one-dimensional multiresolution approximation space $V_j^1$ and $V_j^2$. So the tensor product subspace $F_j = V_j^1 \otimes V_j^2$, and the scaling functions are

$$\varphi = \varphi_1 \otimes \varphi_2 \tag{6}$$

where $\varphi_1 = \{\phi^j_{m,-m+1}(\xi)\phi^j_{m,-m+2}(\xi)\ldots\phi^j_{m,2^j-1}(\xi)\}$ is the one row vector combined by the scaling functions for $m$ at the scale $j$ and $\varphi_2 = \{\phi^j_{m,-m+1}(\eta)\phi^j_{m,-m+2}(\eta)\ldots\phi^j_{m,2^j-1}(\eta)\}$ is the other row vector combined by the scaling functions for $m$ at the scale $j$. $\otimes$ is the kronecker symbol.

The wavelet functions are $\psi^1 = \varphi_1 \otimes \psi_2$, $\psi^2 = \psi_1 \otimes \varphi_2$ and $\psi^3 = \psi_1 \otimes \psi_2$. Fig. 2 shows all the tensor product BSWI scaling functions, which are generated by the one-dimensional BSWI for $m = 4$ at the scale $j = 3$.

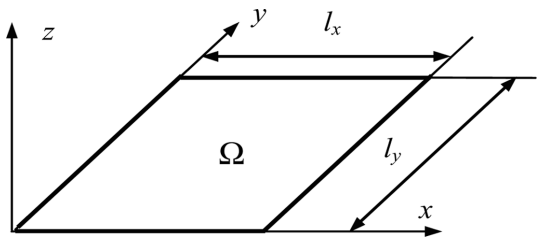


Fig. 3 The solving domain Ω of the rectangle thin plate bending problem

## 3. Thin plate bending and vibration problems

### *3.1 rectangle thin plate FEM BSWI formulation*

Fig. 3 shows the solving domain Ω of the thin plate bending problems.

Based on the classical Kirchoff plate theory assumptions, the generalized function of potential energy for a thin plate is (Zienkiewicz 1988)

$$\Pi_p = \frac{1}{2}\int_{\Omega}\int \boldsymbol{\kappa}^T \mathbf{D}\boldsymbol{\kappa}\mathrm{d}x\mathrm{d}y - \int_{\Omega}\int w\mathrm{q}(x,y)\mathrm{d}x\mathrm{d}y \tag{7}$$

where Ω denote solving domain of thin plate, $q$ is uniform load, $w$ is displacement field function, $\boldsymbol{\kappa}$ is the generalized strain as follow

$$\boldsymbol{\kappa} = \left\{ -\frac{\partial^2 w}{\partial x^2} \quad -\frac{\partial^2 w}{\partial y^2} \quad -2\frac{\partial^2 w}{\partial x \partial y} \right\}^T \tag{8}$$

and the elastic matrix $\mathbf{D}$ is given by

$$\mathbf{D} = D_0 \begin{bmatrix} 1 & \mu & 0 \\ \mu & 1 & 0 \\ 0 & 0 & (1-\mu)/2 \end{bmatrix} \tag{9}$$

in which $\mu$ denotes Poisson's ratio, and the bending stiffness $D_0$ defined by

$$D_0 = \frac{Et^3}{12(1-\mu^2)} \tag{10}$$

where $E$ denotes Young's modulus, and $t$ is the thickness of the thin plate.

If the tensor product BSWI scaling functions are applied to solve the thin plate bending problems, the displacement field function $w$ is interpolated by

$$w = \boldsymbol{\varphi}\mathbf{a} \tag{11}$$

where $\boldsymbol{\varphi}$ is given by Eq. (6) and the unknown wavelet coefficients column vector are

$$\mathbf{a} = \{a_1 \quad a_2 \quad a_3 \ldots a_{(2^j+m-1)(2^j+m-1)}\}^T \tag{12}$$

Substituting Eq. (11) into Eq. (8), we obtain

$$\boldsymbol{\kappa} = \begin{bmatrix} -\dfrac{\partial^2 \boldsymbol{\varphi}_1}{\partial x^2} \otimes \boldsymbol{\varphi}_2 \boldsymbol{\alpha} \\ -\boldsymbol{\varphi}_1 \otimes \dfrac{\partial^2 \boldsymbol{\varphi}_2}{\partial y^2} \mathbf{a} \\ -2\dfrac{\partial \boldsymbol{\varphi}_1}{\partial x} \otimes \dfrac{\partial \boldsymbol{\varphi}_2}{\partial y} \mathbf{a} \end{bmatrix} \tag{13}$$

Substituting Eqs. (9), (11) and (13) into Eq. (7), we have

$$\begin{aligned} \Pi_P = \frac{D_0}{2} \mathbf{a}^T \{ & \mathbf{A}_1^{22} \otimes \mathbf{A}_2^{00} + \mu \mathbf{A}_1^{02} \otimes \mathbf{A}_2^{20} + \mu \mathbf{A}_1^{20} \otimes \mathbf{A}_2^{02} + \mathbf{A}_1^{00} \otimes \mathbf{A}_2^{22} + \\ & 2(1-\mu) \mathbf{A}_1^{11} \otimes \mathbf{A}_2^{11} \} \mathbf{a} - l_x l_y \int_0^1 \int_0^1 q(\xi, \eta) \boldsymbol{\varphi}_1 \otimes \boldsymbol{\varphi}_2 \mathrm{d}\xi \mathrm{d}\eta \end{aligned} \tag{14}$$

where $\mathbf{A}_1^{22} = 1/l_x^3 \int_0^1 \left( \dfrac{\mathrm{d}^2 \boldsymbol{\varphi}_1}{\mathrm{d}\xi^2} \right)^T \left( \dfrac{\mathrm{d}^2 \boldsymbol{\varphi}_1}{\mathrm{d}\xi^2} \right) \mathrm{d}\xi$, $\mathbf{A}_1^{02} = 1/l_x \int_0^1 (\boldsymbol{\varphi}_1)^T \left( \dfrac{\mathrm{d}^2 \boldsymbol{\varphi}_1}{\mathrm{d}\xi^2} \right) \mathrm{d}\xi$, $\mathbf{A}_1^{20} = (\mathbf{A}_1^{02})^T$

$\mathbf{A}_1^{11} = 1/l_x \int_0^1 \left( \dfrac{\mathrm{d}\boldsymbol{\varphi}_1}{\mathrm{d}\xi} \right)^T \left( \dfrac{\mathrm{d}\boldsymbol{\varphi}_1}{\mathrm{d}\xi} \right) \mathrm{d}\xi$, $\mathbf{A}_1^{00} = l_x \int_0^1 (\boldsymbol{\varphi}_1)^T (\boldsymbol{\varphi}_1) \mathrm{d}\xi$

$\mathbf{A}_2^{ij} (i, j = 0, 1, 2)$ are similar to $\mathbf{A}_1^{ij} (i, j = 0, 1, 2)$ if $l_x$ and $\mathrm{d}\xi$ are replaced by $l_y$ and $\mathrm{d}\eta$ respectively.

According to variation principle, let $\delta \Pi_p = 0$, we can obtain FEM BSWI solving equations

$$\mathbf{K}\mathbf{a} = \mathbf{P} \tag{15}$$

where

$$\mathbf{K} = D_0 \{ \mathbf{A}_1^{22} \otimes \mathbf{A}_2^{00} + \mu \mathbf{A}_1^{02} \otimes \mathbf{A}_2^{20} + \mu \mathbf{A}_1^{20} \otimes \mathbf{A}_2^{02} + \mathbf{A}_1^{00} \otimes \mathbf{A}_2^{22} + 2(1-\mu) \mathbf{A}_1^{11} \otimes \mathbf{A}_2^{11} \} \tag{16}$$

and the uniform load column vector is

$$\mathbf{P} = l_x l_y \int_0^1 \int_0^1 q(\xi, \eta) \boldsymbol{\varphi}_1^T \otimes \boldsymbol{\varphi}_2^T \mathrm{d}\xi \mathrm{d}\eta \tag{17}$$

The thin plate displacement can be calculated by Eq. (11) as long as the wavelet coefficients are solved by Eq. (15). According to elastic theory, the moments can be calculated by

$$\mathbf{M} = \mathbf{D}\boldsymbol{\kappa} \tag{18}$$

where $\mathbf{M} = \{M_x \quad M_y \quad M_{xy}\}^T$.

Substituting Eqs. (9) and (13) into Eq. (18), we have

$$\mathbf{M} = -D_0 \begin{bmatrix} \dfrac{1}{l_x^2}\dfrac{\partial^2 \varphi_1}{\partial \xi^2} \otimes \varphi_2 + \dfrac{\mu}{l_y^2}\varphi_1 \otimes \dfrac{\partial^2 \varphi_2}{\partial \eta^2} \\ \dfrac{\mu}{l_x^2}\dfrac{\partial^2 \varphi_1}{\partial \xi^2} \otimes \varphi_2 + \dfrac{1}{l_y^2}\varphi_1 \otimes \dfrac{\partial^2 \varphi_2}{\partial \eta^2} \\ (1-\mu)\dfrac{1}{l_x l_y}\dfrac{\partial \varphi_1}{\partial \xi} \otimes \dfrac{\partial \varphi_2}{\partial \eta} \end{bmatrix} \mathbf{a} \tag{19}$$

### *3.2 skew plate FEM BSWI formulation*

Fig. 4 shows the solving domain Ω of the skew plate bending problems.

When the FEM BSWI is applied to solve the skew plate bending problems, the skew coordinate system is need. The relationship between skew and global coordinate system is

$$\begin{bmatrix} x \\ y \end{bmatrix} = \begin{bmatrix} 1 & -c\tan\alpha \\ 0 & 1/\sin\alpha \end{bmatrix} \begin{bmatrix} \overline{x} \\ \overline{y} \end{bmatrix} \tag{20}$$

In global coordinate system, the generalized function of potential energy for a skew plate is (Shen 1991)

$$\Pi_p = \frac{D_0}{2}\iint_{\Omega}\left\{\left(\frac{\partial^2 w}{\partial \overline{x}^2}+\frac{\partial^2 w}{\partial \overline{y}^2}\right)^2 - 2(1-\mu)\left[\frac{\partial^2 w}{\partial \overline{x}^2}\frac{\partial^2 w}{\partial \overline{y}^2} - \left(\frac{\partial^2 w}{\partial \overline{x}\partial \overline{y}}\right)^2\right]\right\} \mathrm{d}\overline{x}\mathrm{d}\overline{y} - \iint_{\Omega} q(\overline{x}, \overline{y}) w \mathrm{d}\overline{x}\mathrm{d}\overline{y} \tag{21}$$

The displacement field functions $w$ is interpolated by

$$w = \boldsymbol{\varphi}\mathbf{a}_s \tag{22}$$

where $\boldsymbol{\varphi}$ is given by Eq. (6) and the unknown wavelet coefficients column vector is

$$\mathbf{a}_s = \{a_1^s \;\; a_2^s \;\; a_3^s \ldots a_{(2^j+m-1)(2^j+m-1)}^s\}^T \tag{23}$$

Substituting Eqs. (20) and (22) into Eq. (21) and according to variation principle, let $\delta\Pi_p = 0$, we can obtain FEM BSWI solving equations

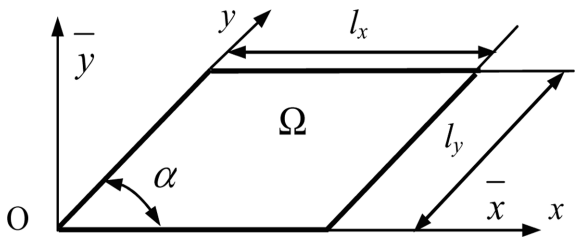


Fig. 4 The solving domain Ω of the skew plate bending problem

$$\mathbf{K}_s \mathbf{a}_s = \mathbf{P}_s \tag{24}$$

where

$$\mathbf{K}_s = \frac{D_0}{\sin^3\alpha}\{\mathbf{A}_1^{22}\otimes\mathbf{A}_2^{00} + \mathbf{A}_1^{00}\otimes\mathbf{A}_2^{22} - 2\cos\alpha(\mathbf{A}_1^{12}\otimes\mathbf{A}_2^{10} + \mathbf{A}_1^{01}\otimes\mathbf{A}_2^{21} + \mathbf{A}_1^{21}\otimes\mathbf{A}_2^{01} + \mathbf{A}_1^{10}\otimes\mathbf{A}_2^{12}) + 2(1-\mu\sin^2\alpha+\cos^2\alpha)\mathbf{A}_1^{11}\otimes\mathbf{A}_2^{11} + (\mu\sin^2\alpha+\cos^2\alpha)(\mathbf{A}_1^{20}\otimes\mathbf{A}_2^{02} + \mathbf{A}_1^{02}\otimes\mathbf{A}_2^{20})\} \tag{25}$$

and the uniform load vector is

$$\mathbf{P}_s = \sin\alpha\, l_x l_y \int_0^1\int_0^1 q(\xi,\eta)\boldsymbol{\varphi}_1^T\otimes\boldsymbol{\varphi}_2^T \mathrm{d}\xi\mathrm{d}\eta \tag{26}$$

in which

$$\mathbf{A}_1^{10} = \int_0^1\left(\frac{\mathrm{d}\boldsymbol{\varphi}_1}{\mathrm{d}\xi}\right)^T(\boldsymbol{\varphi}_1)\mathrm{d}\xi,\ \mathbf{A}_1^{12} = 1/l_x^2\int_0^1\left(\frac{\mathrm{d}\boldsymbol{\varphi}_1}{\mathrm{d}\xi}\right)^T\left(\frac{\mathrm{d}^2\boldsymbol{\varphi}_1}{\mathrm{d}\xi^2}\right)\mathrm{d}\xi,\ \mathbf{A}_0^{01} = (\mathbf{A}_1^{10})^T,\ \mathbf{A}_1^{21} = (\mathbf{A}_1^{12})^T$$

and the other integrations are similar to Eq. (14).

The moments can be calculated by

$$M_x^s = -D_0\left\{\frac{1}{l_x^2}\frac{\partial^2\boldsymbol{\varphi}_1}{\partial\xi^2}\otimes\boldsymbol{\varphi}_2 + \frac{\mu}{\sin^2\alpha}\left(\frac{1}{l_y^2}\boldsymbol{\varphi}_1\otimes\frac{\partial^2\boldsymbol{\varphi}_2}{\partial\eta^2} - \frac{2\cos\alpha}{l_x l_y}\frac{\partial\boldsymbol{\varphi}_1}{\partial\xi}\otimes\frac{\partial\boldsymbol{\varphi}_2}{\partial\eta} + \frac{\cos^2\alpha}{l_x^2}\frac{\partial^2\boldsymbol{\varphi}_1}{\partial\xi^2}\otimes\boldsymbol{\varphi}_2\right)\right\}\mathbf{a}_s \tag{27}$$

$$M_y^s = -D_0\left\{\frac{\mu}{l_x^2}\frac{\partial^2\boldsymbol{\varphi}_1}{\partial\xi^2}\otimes\boldsymbol{\varphi}_2 + \frac{1}{\sin^2\alpha}\left(\frac{1}{l_y^2}\boldsymbol{\varphi}_1\otimes\frac{\partial^2\boldsymbol{\varphi}_2}{\partial\eta^2} - \frac{2\cos\alpha}{l_x l_y}\frac{\partial\boldsymbol{\varphi}_1}{\partial\xi}\otimes\frac{\partial\boldsymbol{\varphi}_2}{\partial\eta} + \frac{\cos^2\alpha}{l_x^2}\frac{\partial^2\boldsymbol{\varphi}_1}{\partial\xi^2}\otimes\boldsymbol{\varphi}_2\right)\right\}\mathbf{a}_s \tag{28}$$

and

$$M_{xy}^s = -\frac{D_0(1-\mu)}{\sin\alpha}\left\{\frac{1}{l_x l_y}\frac{\partial\boldsymbol{\varphi}_1}{\partial\xi}\otimes\frac{\partial\boldsymbol{\varphi}_2}{\partial\eta} - \frac{\cos\alpha}{l_x^2}\frac{\partial^2\boldsymbol{\varphi}_1}{\partial\xi^2}\otimes\boldsymbol{\varphi}_2\right\}\mathbf{a}_s \tag{29}$$

### 3.3 FEM BSWI for thin plate free vibration problems

The generalized function of potential energy for the rectangle thin plate free vibration problem is (Zienkiewicz 1988)

$$\Pi_p = \frac{1}{2}\int_\Omega\int\boldsymbol{\kappa}^T\mathbf{D}\boldsymbol{\kappa}\mathrm{d}x\mathrm{d}y - \frac{1}{2}\int_\Omega\int\rho t\omega^2 w^T w\mathrm{d}x\mathrm{d}y \tag{30}$$

where $\rho$ is the density and $\omega$ is the circular frequency.

Similarly to the procedures of section 3.1, we have the free vibration frequency equations for rectangle thin plate vibration problem

$$\left|\mathbf{K}-\omega^2\mathbf{M}\right| = 0 \tag{31}$$

where $\mathbf{K}$ is stiffness matrix as shown in Eq. (16) and $\mathbf{M}$ is the consistent mass matrix that can be obtained from

$$\mathbf{M} = l_x l_y \rho t \mathbf{A}_1^{00} \otimes \mathbf{A}_2^{00} \tag{32}$$

The free vibration frequency equations for skew plate vibration problem are given by

$$\left| \mathbf{K}_s - \omega^2 \mathbf{M}_s \right| = 0 \tag{33}$$

where $\mathbf{K}_s$ is stiffness matrix, as shown in Eq. (25). $\mathbf{M}_s$ is the consistent mass matrix that can be obtained by

$$\mathbf{M}_s = \sin\alpha l_x l_y \rho t \mathbf{A}_1^{00} \otimes \mathbf{A}_2^{00} \tag{34}$$

## 4. Numerical examples

A number of examples are taken to examine the performance of the FEM BSWI, which include the rectangle and skew thin plate bending problems for various boundary conditions subjected to uniform or concentrated load and the rectangle and skew thin plate free vibration problems. The numerical results are compared with those obtained by other analytical or numerical method. In this section, the tensor product BSWI scaling functions for $m = 4$ at the scale $j = 3$ are adopted to build FEM BSWI solving equations. Supposing Poisson's ratio $\mu = 0.3$ for all examples. The order of stiffness matrix, which is given by Eq. (16), Eq. (25), Eq. (30) or Eq. (33) is $121 \times 121$ when the tensor product BSWI scaling functions for $m = 4$ at the scale $j = 3$ are adopted to build FEM BSWI equations.

### *4.1 Example 1: Square plate*

A square plate, which is subjected to a uniformly distributed load or a concentrated load is modeled with four different boundary conditions, i.e. case 1: clamped boundary conditions on all four sides (CCCC), case2: simply supported boundary conditions on all four sides (SSSS), case3: simply supported boundary conditions on two opposite sides and the other two opposite sides are clamped (SCSC) and case4: clamped boundary conditions on one side and the other three sides are simply supported (CSSS).

Table 1 shows the results of the central displacement and moments, obtained by FEM BSWI, for uniform and concentrated loads, where $q$ is the uniformly distributed load, $P$ is the concentrated load and $L$ is the length of the square plate. The displacement results obtained by the presented formulation are in good agreement with closed-form solutions. However, for the sake of differential operations, the relative errors of moments are much poor than those of displacement.

Fig. 5(a) shows deformation of square plate for simply supported boundary conditions on all four sides. The contour plots of the deformed plate along $x$ direction are shown in Fig. 5(b), the bottom line is the deformation of middle line along $x$ direction and the upper line is the simply supported side.

Table 2 shows the FEM BSWI results of the central displacement $w100D_0/q_0L^4$, central moment $M_x 10/q_0L^2$ and torque moment $M_{xy}10/q_0L^2$ of the corner points obtained by FEM BSWI, for

Table 1 Central displacements and moments of square plate for various boundary conditions subjected to uniform and concentrated loads (Timoshenko 1970)

| Case | Method | Uniform load | | | Concentrated load | | |
|---|---|---|---|---|---|---|---|
| | | $w100D_0/qL^4$ | $M_x10/qL^2$ | $M_y10/qL^2$ | $wD_0100/PL^2$ | $M_x10/P$ | $M_y10/P$ |
| 1 | BSWI | 0.12652 | 0.23288 | 0.23288 | 0.55698 | 2.76529 | 2.76529 |
| | Exact | 0.12652 | 0.2310 | 0.2310 | 0.56120 | – | – |
| | Error (%) | 0 | 1.67255 | 1.67255 | 0.75196 | – | – |
| 2 | BSWI | 0.40625 | 0.48136 | 0.48136 | 1.15591 | 3.30127 | 3.30127 |
| | Exact | 0.4062 | 0.4789 | 0.4789 | 1.1600 | – | – |
| | Error (%) | 0.01231 | 0.51368 | 0.51368 | 0.35259 | – | – |
| 3 | BSWI | 0.1917 | 0.24530 | 0.33899 | 0.6998 | 2.79264 | 3.00078 |
| | Exact | 0.192 | 0.244 | 0.332 | – | – | – |
| | Error (%) | 0.15625 | 0.53279 | 2.10542 | – | – | – |
| 4 | BSWI | 0.27970 | 0.34070 | 0.39668 | 0.7987 | 2.99893 | 3.12238 |
| | Exact | 0.28 | 0.34 | 0.39 | – | – | – |
| | Error (%) | 0.10714 | 0.20588 | 1.71282 | – | – | – |

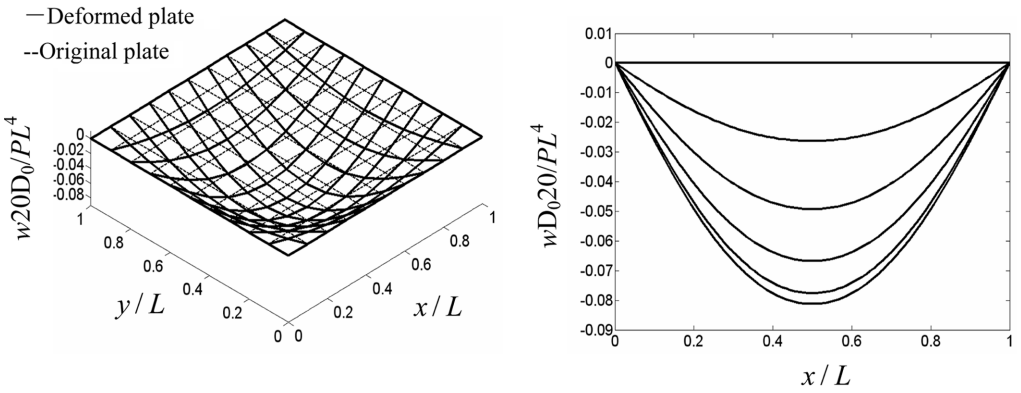


(a) Deformed plate (b) Contour plots along $x$ direction

Fig. 5 The deformation of square plate for simply supported boundary conditions on all four sides

Table 2 Central displacements and moments of square plate for simply supported boundary condition on all four sides subjected to distributed load (Timoshenko 1970)

| Method | $w100D_0/q_0L^4$ | $M_x10/q_0L^2$ | $M_{xy}10/q_0L^2$ |
|---|---|---|---|
| BSWI | 0.25666 | 0.33357 | 0.17732 |
| Exact | 0.25665 | 0.32930 | 0.18041 |
| Error (%) | 0.00390 | 1.29669 | 1.71277 |

distributed load $q = q_0 \sin\frac{\pi x}{L} \times \sin\frac{\pi y}{L}$, where $q_0$ is the uniformly distributed load. The results obtained by the presented method have good accuracy compared with the closed-form solutions.

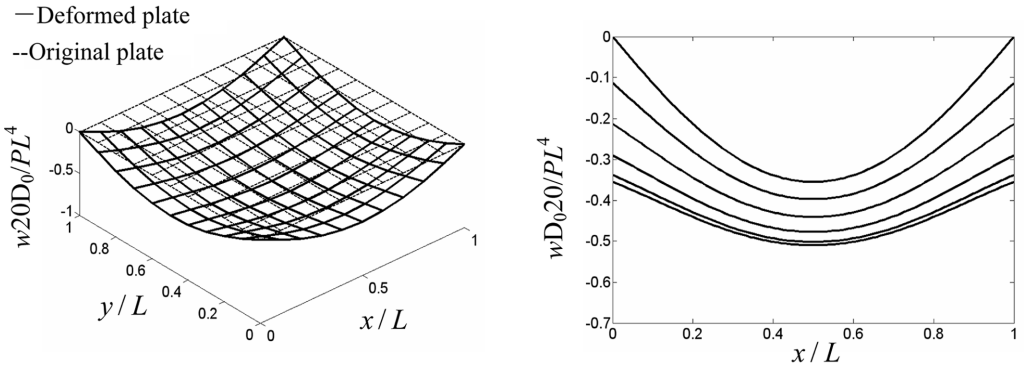


(a) Deformed plate (b) Contour plots along $x$ direction

Fig. 6 The deformation of square plate for corner point supported on all four-corner points subjected to uniform load

Fig. 6(a) shows deformation of square plate for corner point supported boundary conditions on all four-corner point subjected to uniform load. The contour plots of the deformed plate along $x$ direction are shown in Fig. 6(b), the bottom line is the deformation of middle line along $x$ direction and the upper line is the back edge.

### *4.2 Example 2: Skew plate*

A skew plate (skew angle $\alpha = 60^{o}$) subjected to a uniform load, which is modeled with simply supported boundary conditions on two opposite sides and the other two sides are free (SFSF). Table 3 shows the FEM BSWI results of central displacement and moment and those of the other

Table 3 Comparison of FEM BSWI results of central displacement and moment of the skew plate with those of the other FEM. (SFSF.) (Zienkiewicz 1988)

| (a) Central displacement $w \times 100 \times D_0/qL^4$ | | | | | | | | |
|---|---|---|---|---|---|---|---|---|
| Mesh | BSWI | DKQ | ACQ | LSL-Q12 | MITC4 | MiSP4 | MMiSP4 | DSQ |
| 8 × 8 | – | 0.7876 | 0.7920 | 0.7918 | 0.7610 | 0.7781 | 0.7604 | 0.7840 |
| 10 × 10 | 0.7925 | – | – | – | – | – | – | – |
| 12 × 12 | – | 0.7909 | 0.7927 | 0.7927 | 0.7785 | – | – | – |
| 16 × 16 | – | 0.7920 | 0.7930 | – | – | 0.7894 | 0.7832 | 0.7871 |
| Exact | | | | 0.7945 | | | | |
| (b) Central moment $M_y \times 10/qL^2$ | | | | | | | | |
| Mesh | BSWI | DKQ | ACQ | LSL-Q12 | MITC4 | MiSP4 | MMiSP4 | DSQ |
| 8 × 8 | – | 0.9605 | 0.9990 | 0.9777 | 0.9090 | 0.9423 | 0.9052 | 0.9609 |
| 10 × 10 | 0.9715 | – | – | – | – | – | – | – |
| 12 × 12 | – | 0.9602 | 0.9777 | 0.9680 | 0.9370 | – | – | – |
| 16 × 16 | – | 0.9601 | 0.9700 | – | – | 0.9567 | 0.9466 | 0.9602 |
| Exact | | | | 0.9589 | | | | |

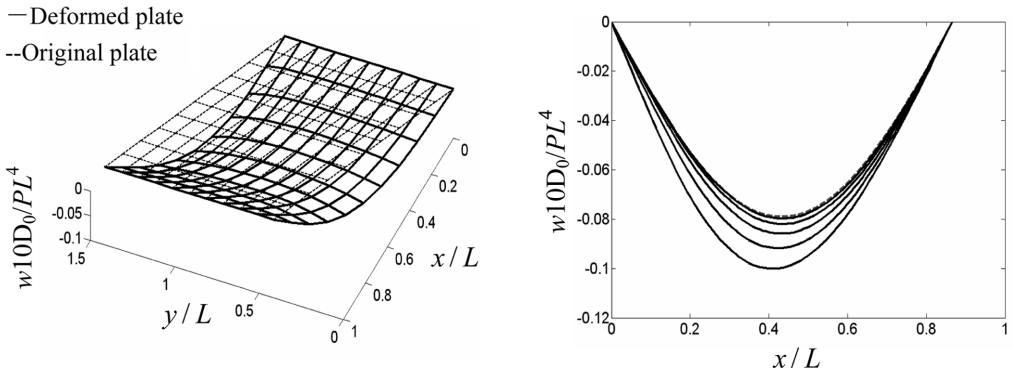


(a) Deformed plate (b) Contour plots along $x$ direction

Fig. 7 The deformation of skew plate for SFSF subjected to uniform load

Table 4 Central displacement $w \times 1000 \times D_0/qL^4$ of skew plates for simply supported or clamped boundary conditions at all four sides (GangaRao 1988, Morley 1963)

| Skew angle $\alpha$ | Simply supported skew plate subjected to uniform load of intensity $q$ | | | Clamped skew plate subjected to uniform load of intensity $q$ | | |
|---|---|---|---|---|---|---|
| | BSWI | GangaRao | Morley | BSWI | GangaRao | Morley |
| 90° | 4.0625 | 4.06 | 4.06 | 1.2652 | 1.27 | 1.26 |
| 85° | 4.0134 | 4.01 | 4.01 | 1.2487 | – | – |
| 80° | 3.8683 | 3.87 | 3.87 | 1.2002 | 1.20 | 1.20 |
| 75° | 3.6343 | 3.64 | – | 1.1226 | – | – |
| 70° | 3.3228 | – | – | 1.0206 | 1.02 | 1.02 |
| 60° | 2.5419 | 2.56 | 2.56 | 0.7680 | 0.771 | 0.769 |
| 55° | 2.0929 | 2.14 | | 0.6317 | – | – |
| 50° | 1.6955 | 1.72 | 1.72 | 0.4982 | 0.503 | 0.500 |
| 45° | 1.2830 | 1.32 | – | 0.3741 | – | – |
| 40° | 0.9264 | 0.958 | 0.958 | 0.2648 | 0.269 | 0.270 |
| 30° | 0.3883 | 0.406 | 0.408 | 0.1039 | 0.108 | – |

FEM. Both the displacement and moment results indicate the FEM BSWI have higher accuracy and less meshes.

Fig. 7(a) shows deformation of skew plate for SFSF, which is subjected to uniform load. The contour plots of the deformed plate along $x$ direction are shown in Fig. 7(b), the deformation of middle line along $x$ direction is shown as dashed.

Table 4 shows results of the FEM BSWI and the other methods of a skew plate, which is subjected to a uniform load under two different boundary conditions, i.e. simply supported and clamped boundary on all four sides. The skew angle $\alpha$ is chosen from 30 to 90 degree. The FEM BSWI solutions are match well with those of the other methods.

### 4.3 Example 3: Free vibration for thin plate

Firstly, we use FEM BSWI to analysis the free vibration problem of a square plate for various

boundary conditions i.e. case1, case2, case3 and case4, which is similar to example 1. The first five non-dimensional natural frequencies $\Omega_i (i = 1, 2, \ldots, 5)$ solved by FEM BSWI and other analytical methods are shown in Table 5. The accuracy of FEM BSWI is very high.

Fig. 8 shows the first six-mode shapes of thin plate for clamped boundary on all four edges.

Secondly, the free vibration problem of a skew plate is also given. Table 6 gives the non-dimensional natural frequencies $\lambda_i (i = 1, 2, \ldots, 5)$ of the skew plate for various boundary conditions, i.e. case 1: clamped boundary conditions on all four sides (CCCC), case2: simply supported boundary conditions on all four sides (SSSS), case3: simply supported boundary

Table 5 The first five natural frequencies of rectangle square plate for various boundary conditions (Frequency parameters $\Omega_i = \omega_i L^2 (\rho t / D_0)^{1/2}$ ).( Blevins 1979, Warburton 1954)

| case | Method | $\Omega_1$ (rad/s) | $\Omega_2$ (rad/s) | $\Omega_3$ (rad/s) | $\Omega_4$ (rad/s) | $\Omega_5$ (rad/s) |
|---|---|---|---|---|---|---|
| 1 | BSWI | 35.9915 | 73.4457 | 73.4457 | 108.3172 | 131.9954 |
| | Exact | 35.99 | 73.41 | – | 108.3 | 131.6 |
| | Error (%) | 0.0042 | 0.0486 | – | 0.0159 | 0.3005 |
| 2 | BSWI | 19.7394 | 49.3575 | 49.3575 | 78.9689 | 98.8359 |
| | Exact | 19.74 | 49.35 | – | 78.95 | 98.64 |
| | Error (%) | 0.0030 | 0.0152 | – | 0.0239 | 0.1986 |
| 3 | BSWI | 28.9532 | 54.7601 | 69.3689 | 94.6373 | 102.3746 |
| | Exact | 28.95 | 54.74 | 69.32 | 94.59 | 102.2 |
| | Error (%) | 0.0111 | 0.0367 | 0.0705 | 0.0500 | 0.1708 |
| 4 | BSWI | 23.6471 | 51.6865 | 58.6675 | 86.1621 | 100.4169 |
| | Exact | 23.64 | 51.67 | 58.65 | 86.12 | 100.30 |
| | Error (%) | 0.0300 | 0.0319 | 0.0298 | 0.0489 | 0.1166 |

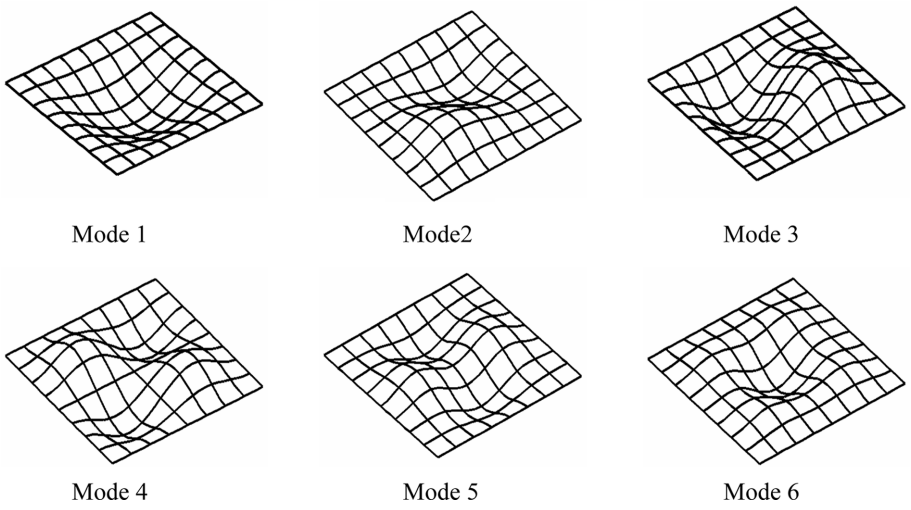


Fig. 8 The mode shapes of thin plate for clamped boundary on all four edges

Table 6 The first five natural frequencies of skew plate for various boundary conditions (Frequency parameters $\lambda_i = (\omega_i L^2/\pi^2)(\rho t/D_0)^{1/2}$)

| Case | Skew angle $\alpha$ | 90° | 75° | 60° | 45° | 30° |
|---|---|---|---|---|---|---|
| 1 (CCCC) | $\lambda_1$ | 3.6467 | 3.8702 | 4.6751 | 6.6854 | 12.6068 |
| | $\lambda_2$ | 7.4416 | 7.3926 | 8.2850 | 10.8734 | 18.7711 |
| | $\lambda_3$ | 7.4416 | 8.3810 | 10.6963 | 15.3670 | 25.9691 |
| | $\lambda_4$ | 10.9748 | 11.1230 | 12.1546 | 16.1455 | 32.1820 |
| | $\lambda_5$ | 13.3739 | 14.1385 | 16.8948 | 20.9490 | 35.6906 |
| 2 (SSSS) | $\lambda_1$ | 2.0000 | 2.1154 | 2.5371 | 3.6231 | 6.9105 |
| | $\lambda_2$ | 5.0010 | 4.8853 | 5.3357 | 6.7262 | 10.7707 |
| | $\lambda_3$ | 5.0010 | 5.6886 | 7.3029 | 10.2478 | 15.6684 |
| | $\lambda_4$ | 8.0012 | 8.0137 | 8.5129 | 11.0790 | 21.7654 |
| | $\lambda_5$ | 10.0142 | 10.5555 | 12.4840 | 14.5090 | 22.1514 |
| 3 (SCSC) | $\lambda_1$ | 2.9336 | 3.1112 | 3.7530 | 5.3669 | 10.1524 |
| | $\lambda_2$ | 5.5484 | 5.7485 | 6.5226 | 8.5179 | 14.3698 |
| | $\lambda_3$ | 7.0285 | 7.5687 | 9.4602 | 12.6589 | 20.4279 |
| | $\lambda_4$ | 9.5888 | 9.5410 | 10.2476 | 14.1040 | 26.9970 |
| | $\lambda_5$ | 10.3727 | 11.3725 | 14.0355 | 17.5510 | 29.2222 |
| 4 (CFFF) | $\lambda_1$ | 0.3518 | 0.3633 | 0.3986 | 0.4584 | 0.5431 |
| | $\lambda_2$ | 0.8623 | 0.8816 | 0.9552 | 1.1483 | 1.6489 |
| | $\lambda_3$ | 2.1577 | 2.2536 | 2.5671 | 2.7487 | 3.2043 |
| | $\lambda_4$ | 2.7564 | 2.6691 | 2.6295 | 3.2230 | 4.7242 |
| | $\lambda_5$ | 3.1384 | 3.4332 | 4.1946 | 5.1525 | 6.1515 |
| 5(CFCF) | $\lambda_1$ | 2.2478 | 2.3672 | 2.7803 | 3.7266 | 6.1783 |
| | $\lambda_2$ | 2.6785 | 2.7724 | 3.1071 | 3.9226 | 6.2353 |
| | $\lambda_3$ | 4.4206 | 4.5485 | 5.0330 | 6.3018 | 10.1236 |
| | $\lambda_4$ | 6.2065 | 6.5448 | 7.5216 | 8.9463 | 12.9032 |
| | $\lambda_5$ | 6.8166 | 7.1445 | 8.2662 | 10.7022 | 16.5606 |
| 6(SFSF) | $\lambda_1$ | 0.9759 | 1.0334 | 1.2317 | 1.6721 | 2.6477 |
| | $\lambda_2$ | 1.6348 | 1.6708 | 1.7970 | 2.0872 | 2.8062 |
| | $\lambda_3$ | 3.7217 | 3.6465 | 3.6518 | 4.0210 | 5.5009 |
| | $\lambda_4$ | 3.9472 | 4.2005 | 5.0128 | 6.0910 | 7.6158 |
| | $\lambda_5$ | 4.7369 | 5.1370 | 6.2297 | 8.0651 | 10.5324 |

conditions on two opposite sides and the other two opposite sides are clamped (SCSC), case4: clamped boundary conditions on one side and the other three sides are free (CFFF), case5: clamped boundary conditions on two opposite sides and the other two opposite sides are free (CFCF) and case6: simply supported boundary conditions on two opposite sides and the other two opposite sides are free (SFSF).

To validate the accuracy of FEM BSWI, the non-dimensional fundamental frequency $\lambda_1$ of the skew plates for various boundary conditions has been compared with those obtained by Raju (1980) and Liew (1993), as shown in Table 7. The difference between two results is negligible. From these results, it may be noted that the proposed FEM BSWI gives the reliable and accurate solutions

Table 7 Comparison of non-dimensional fundamental frequency ($\lambda_1$) of thin skew plate for various boundary conditions. (Raju 1980, Liew 1993)

| Case | Method | Fundamental frequency for skew plate angles | | | | |
|---|---|---|---|---|---|---|
| | | 90° | 75° | 60° | 45° | 30° |
| 1 (CCCC) | Raju | 3.6481 | 3.8716 | 4.6744 | 6.6652 | 12.4080 |
| | Present | 3.6467 | 3.8702 | 4.6751 | 6.6854 | 12.6068 |
| 2 (SSSS) | Raju | 2.0006 | 2.1172 | 2.5479 | 3.6664 | 7.0582 |
| | Present | 2.0000 | 2.1154 | 2.5371 | 3.6231 | 6.9105 |
| 3 (SCSC) | Raju | 2.9347 | 3.1122 | 3.7497 | 5.3300 | 9.8868 |
| | Present | 2.9336 | 3.1112 | 3.7530 | 5.3669 | 10.1524 |
| 4 (CFFF) | Liew | 0.3517 | 0.3631 | 0.3983 | 0.4571 | 0.5346 |
| | Present | 0.3518 | 0.3633 | 0.3986 | 0.4584 | 0.5431 |
| 5 (CFCF) | Liew | 2.2462 | 2.3656 | 2.7763 | 3.6933 | 5.8584 |
| | Present | 2.2478 | 2.3672 | 2.7803 | 3.7266 | 6.1783 |
| 6 (SFSF) | Liew | 0.9759 | 1.0334 | 1.2310 | 1.6649 | 2.5810 |
| | Present | 0.9759 | 1.0334 | 1.2317 | 1.6721 | 2.6477 |

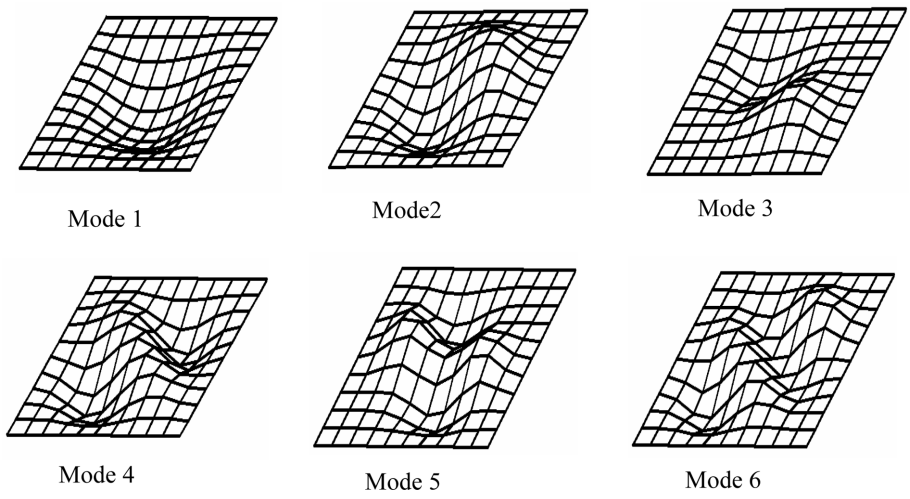


Fig. 9 The mode shape of skew plate for simply supported boundary conditions on all four edges

regardless of the higher corner singularity due to the decreased of skew angles and geometric constraints.

Fig. 9 gives the first six-mode shapes of skew plate for simply supported boundary conditions on all four edges, where the skew angle $\alpha = 60$.

## 5. Conclusions

Based on the two-dimensional tensor product BSWI, the FEM BSWI solving equations are built

to solve the rectangle and skew plate bending and vibration problems. Because the good character of BSWI scaling functions, the FEM BSWI presented in this paper is a useful tool to deal with high performance computation in engineering. The numerical results are presented in this paper for several well-selected problems demonstrating the accuracy, efficiency and reliability of the method developed herein. It has been noted that the examples used in this paper adopted the tensor product BSWI scaling functions for $m = 4$ at $j = 3$ to form the FEM BSWI solving equations. But the other scaling functions of BSWI such as $m = 4$ at $j = 4, 5, \ldots$, also can be applied to form FEM BSWI equations to get higher accuracy.

Because the built-in hierarchy property of wavelet, which is suitable for a multi-level solution procedures, the future research is the construction of hierarchy FEM BSWI in order to make use of the advantages of wavelets basis functions for approximation in FEM.

## Acknowledgements

This work is supported by the key project of National Natural Science Foundation of China (No.50335030), National Basic Research Program of China (No. 2005CB724106), National Natural Science Foundation of China(No.50505033, 50575171), Doctor Program Foundation of University of China (No. 20040698026) Thanks are also due to the anonymous referees for their helpful comments.

## References

Basu, P.K., Jorge, A.B., Badri, S. and Lin, J. (2003), "Higher-order modeling of continua by finite-element, boundary-element, Meshless, and wavelet methods", *Comput. Math. Appl.*, **46**, 15-33.

Bertoluzza, S., Naldi, G. and Ravel, J.C. (1994), "Wavelet methods for the numerical solution of boundary value problems on the interval", *Wavelets: Theory, Algorithms, and Applications*. Chui, C.K., Montefusco, L. and Puccio, L. (eds.), Academic Press, London. 425-448.

Blevins, R.D. (1979), *Formulas for Natural Frequency and Mode Shape*, Van Nostrand Reinhold Co., New York.

Canuto, C., Tabacco, A. and Urban, K. (1999), "The wavelet element method Part I: Construction and analysis", *Appl. Comput. Harmon. A.*, **6**, 1-52.

Canuto, C., Tabacco, A. and Urban, K. (2000), "The wavelet element method Part II: Realization and additional feature in 2D and 3D", *Appl. Comput. Harmon. A.*, **8**, 123-165.

Chen, W.H. and Wu, C.W. (1995), "A spline wavelets element method for frame structures vibration", *Comput. Mech.*, **16**(1), 11-21.

Chen, W.H. and Wu, C.W. (1996), "Extension of spline wavelets element method to membrane vibration analysis", *Comput. Mech.*, **18**(1), 46-54.

Chen, X.F., Yang, S.J., Ma, J.X. and He, Z.J. (2004), "The construction of wavelet finite element and its application", *Finite Elem. Anal. Des.*, **40**(5-6), 541-554.

Chui, C.K. and Quak, E. (1992), "Wavelets on a bounded interval", *Numer. Math. Approx. Theory*, **1**, 53-57.

Cohen, A. (2003), *Numerical Analysis of Wavelet Method*, Elsevier Press, Amsterdam.

GangaRao, Hota V.S. and Chaudhary, V.K. (1988), "Analysis of skew and triangular plates in bending", *Comput. Struct.*, **28**(2), 223-235.

Goswami, J.C., Chan, A.K. and Chui, C.K. (1995), "On solving first-kind integral equations using wavelets on a bounded interval", *IEEE T. Antenn. Propag.*, **43**, 614-622.

Ko, J., Kurdila, A.J. and Pilant, M.S. (1997), "Triangular wavelet based finite elements via multivalued scaling

equations", *Comput. Meth. Appl. Mech. Eng.*, **146**(1-2), 1-17.
Liew, K.M., Xiang, Y., Kittipornchai, S. and Wang, C.M. (1993), "Vibration of thick skew plates based on Mindlin shear deformation plate theory", *J. Sound Vib.*, **168**(1), 39-69.
Ma, J.X., Xue, J.J., Yang, S.J. and He, Z.J. (2003), "A study of the construction and application of a Daubechies wavelet-based beam element", *Finite Elem. Anal. Des.*, **39**(10), 965-975.
Mallat, S.G. (1999), *A Wavelet Tour of Signal Processing*, Academic Press, London.
Morley, L.S.D. (1963), *Skew Plates and Structures*, Pergamon Press, New York.
Quak, E. and Weyrich, N. (1994), "Decomposition and Reconstruction algorithms for spline wavelets on a Bounded interval", *Appl. Comput. Harmon. A.*, **3**, 217-231.
Raju, K.K. and Hinton, E. (1980), "Natural frequencies and modes of rhombic Mindlin plates", *Earthq. Eng. Struct. Dyn.*, **8**, 55-62.
Shen, P.C. (1991), *Spline Finite Methods in Structural Analysis*, Hydraulic and Electric Press, Beijin (In Chinese).
Shen, P.C. and He, P.X. (1995), "Bending analysis of rectangular moderately thick plates using spline finite element method", *Comput. Struct.*, **54**(6), 1023-1029.
Timoshenko, S.P. and Goodier, J.N. (1970), *Theory of Elasticity*, McGraw-Hill Press, New York.
Warburton, G.B. (1954), "The vibration of rectangular plates", *Proc. of Institution of Mechanical Engineering*, London, 371-385.
Xiang, J.W., Chen, X.F., He, Y.M. and He, Z.J. (2006), "The construction of plane elastomechanics and mindlin plate elements of B-spline wavelet on the interval", *Finite Elem. Anal. Des.*, **42**(14-15), 1269-1280.
Xiang, J.W., Chen, X.F., Li, B., He, Y.M. and He, Z.J. (2006), "Identification of crack in a beam based on finite element method of B-spline wavelet on the interval", *J. Sound Vib.*, **296**(4-5), 1046-1052.
Zhou, Y.H., Wang, J.Z. and Zheng, X.J. (1998), "Application of wavelet Galerkin FEM to bending of beam and plate structures", *Appl. Math. Mech.*, **19**(8), 697-706.
Zienkiewicz, O.C. (1988), *The Finite Element Method*, McGRAW-Hill Book Company Limited, London.
Zienkiewicz, O.C. and Lefebvre, D. (1988), "A robust triangular plate bending element of the Reissener-Mindlin type", *Int. J. Numer. Methods Eng.*, **26**, 1169-1184.